

Modeling Multiple Vias With Arbitrary Shape of Antipads and Pads in High Speed Interconnect Circuits

Boping Wu, *Student Member, IEEE*, and Leung Tsang, *Fellow, IEEE*

Abstract—This letter successfully extends the full-wave semi-analytical approach, based on Foldy–Lax multiple scattering equations and modal expansions, to solve massively-coupled multiple vias with arbitrary shape of antipads and pads in high speed interconnect circuits. The magnetic frill current at the antipad aperture is calculated using finite difference method. Numerical examples of as many as 16-by-16 via array demonstrate that this approach is able to model the multiple vias problem at about five thousand times faster than Ansoft HFSS and yet is within 5% difference of accuracy up to 20 GHz.

Index Terms—Foldy–Lax equation, high-speed interconnects, printed circuit boards (PCBs), signal integrity, via connections.

I. INTRODUCTION

V IAS are one of the key structures in multilayered substrates of high speed interconnect circuits, which aim to provide a new design complexity of vertical integration. Parallel-plate waveguide modes are induced by high frequency signals along vertical vias within layers. Because of multiple scattering among the massively-coupled vias, such interference is usually not localized in space. This poses serious design problems for power integrity and signal integrity.

In the past, a circuit model of complex via structures was proposed [1] using a cascade of capacitance and inductance matrices. An even- and odd-mode decomposition approach [2] was used to account for coupling noise between two adjacent vias. In our research, we used a semi-analytical approach, based on Foldy-Lax scattering equations and modal expansions, to compute the full-wave solution of multiple cylindrical vias in planar waveguides [3]–[5]. The magnetic field Green's functions are expressed in terms of waveguide modes in the vertical direction and vector cylindrical wave expansions in the horizontal direction. This method goes beyond the equivalent circuit models and the analytic decomposition methods. After extraction of equivalent circuits for via structures using solved admittance matrices, system-level SPICE simulations have been demonstrated. Excellent agreements were shown when compared with Ansoft

HFSS simulations [5]. The results were also validated by hardware measurements for the entire board [6]. An approach similar to ours was used in paper [7].

In this letter, we successfully extend this approach to solve the vias with arbitrary shape of antipads and pads by calculating the magnetic frill current at the antipad aperture using finite difference method (FDM). The results are in good agreement with HFSS simulations.

II. FOLDY-LAX EQUATIONS FOR MULTIPLE VIAS SCATTERING

By using the equivalence principle, the antipad apertures can be replaced by a perfect electric conductor (PEC) with magnetic currents at the apertures. The multiple scattering among N via cylinders between two parallel PEC ground/power plates can be formulated in terms of Foldy-Lax multiple scattering equations, which state that the final exciting field of via q is equal to the incident field plus scattered fields from the other vias

$$w_{\text{ln}}^{TM(q)} = a_{\text{ln}}^{TM(q)} + \sum_{\substack{p=1 \\ p \neq q}}^N \sum_{m=-\infty}^{\infty} H_{n-m}^{(2)}(k_{\rho l} |\bar{\rho}_p - \bar{\rho}_q|) \times e^{j(n-m)\phi_{\bar{\rho}_p \bar{\rho}_q}} T_m^{(N)} w_{\text{lm}}^{TM(p)} \quad (1)$$

$$T_m^{(N)} = -J_m(k_{\rho l} a) / H_m^{(2)}(k_{\rho l} a). \quad (2)$$

$w_{\text{ln}}^{TM(q)}$ is the exciting field coefficient to be solved. $a_{\text{ln}}^{TM(q)}$ is the incident field coefficient onto via q and can be calculated by the following equation containing a 2-D integration over the current source:

$$a_{\text{ln}}^{TM(q)} = \frac{\eta j \omega \varepsilon}{2d} \frac{(-1)^{n+l}}{k_{\rho l}^2} f_l \times \int \int d\bar{\rho}' \bar{m}_{-n}(k_{\rho l}, |\bar{\rho}' - \bar{\rho}_q|) e^{jn\phi_{\bar{\rho}' \bar{\rho}_q}} \cdot \bar{M}_s(\bar{\rho}') \quad (3)$$

$$\bar{m}_{-n}(k_{\rho l}, |\bar{\rho}' - \bar{\rho}_q|) = \hat{\rho}_{\bar{\rho}' \bar{\rho}_q} \frac{jn}{|\bar{\rho}' - \bar{\rho}_q|} H_{-n}^{(2)}(k_{\rho l} |\bar{\rho}' - \bar{\rho}_q|) - \hat{\phi}_{\bar{\rho}' \bar{\rho}_q} k_{\rho l} H_{-n}^{(2)'}(k_{\rho l} |\bar{\rho}' - \bar{\rho}_q|) \quad (4)$$

where $\bar{M}_s(\bar{\rho}')$ is the equivalent magnetic surface current at the antipad aperture. The choices of number of waveguide modes l , azimuthal variation order n and m , and the formulae of calculating admittance matrix \mathbf{Y} using exciting field coefficients are described in paper [5].

III. MODELING ARBITRARY SHAPE OF ANTIPAD AND PAD

In the past, we used the model of circular antipad and concentric via drilling. For this case, the magnetic surface current is in

Manuscript received June 20, 2008; revised September 08, 2008. First published December 22, 2008; current version published January 08, 2009. This work was supported by the Semiconductor Research Corporation.

The authors are with the Department of Electrical Engineering, University of Washington-Seattle, Seattle, WA 98195 USA (e-mail: bennywu@u.washington.edu; tsangl@u.washington.edu).

Color versions of one or more of the figures in this letter are available online at <http://ieeexplore.ieee.org>.

Digital Object Identifier 10.1109/LMWC.2008.2008532

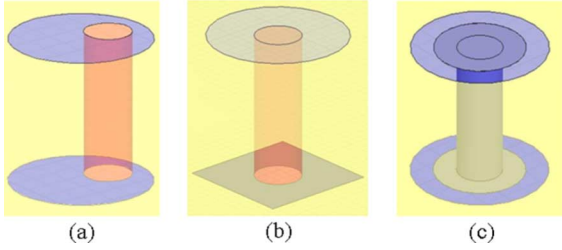


Fig. 1. Via geometry for (a) off-center via drilling in circular antipads, (b) center via drilling in circular antipad on top and squared antipad at bottom, and (c) center via drilling plus circular pads in circular antipads.

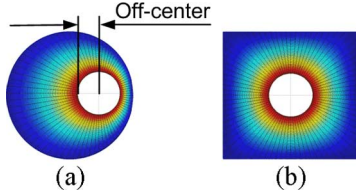


Fig. 2. Potential distribution for apertures of (a) off-center via drilling in circular antipad, and (b) concentric via in squared antipad.

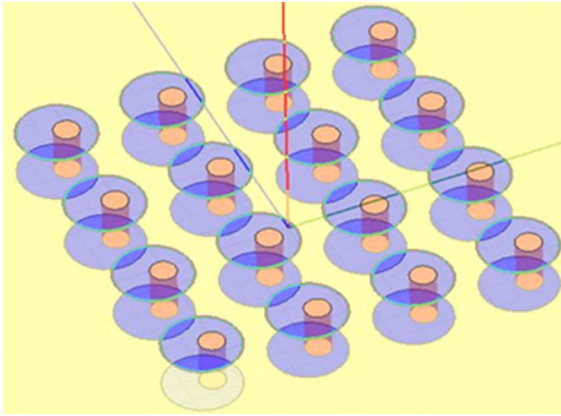


Fig. 3. 4-by-4 via array with 4 mil off-center via drilling.

the circular direction and can be expressed analytically [3]. In the fabrication of printed circuit boards (PCBs) and electronic packages, it is quite common that the via is not drilled exactly at the center of the antipad. Also, the antipad can be non-circular for certain kinds of designs.

In this letter, we assume that the potential distribution in the antipad satisfies an electrostatic 2-D Laplace equation (5) with unit and zero voltages on the two boundaries of the antipad. The FDM is used in Matlab to solve the potential distribution

$$\nabla^2 V = \frac{1}{\rho} \frac{\partial}{\partial \rho} \left(\rho \frac{\partial V}{\partial \rho} \right) + \frac{1}{\rho^2} \frac{\partial^2 V}{\partial \phi^2} = 0. \quad (5)$$

Fig. 2 shows the voltage fields for two different kinds of apertures. The potential distribution is then used to calculate the electric field by $\vec{E} = -\nabla V$. The magnetic frill current is perpendicular to the electric field according to the equation $\vec{M}_s = -\hat{n} \times \vec{E}$. After \vec{M}_s is calculated, we can calculate the incident field coefficients by using (3) and sampling one hundred integration points on the aperture. Using the potential distribution, the surface charge distribution on pad can be calculated and the capacitance C per unit length is also obtained.

TABLE I
CPU OF 20 FREQUENCIES RUN TIME FOR VARIOUS VIA ARRAY SIZES ON ANSOFT HFSS AND FOLDY-LAX APPROACH

Size of via array	Ansoft HFSS	Foldy-Lax
16-by-16	388'800 sec. (4.5 days)	73 sec.
8-by-8	26'700 sec. (7.3 hr.)	4.54 sec.
4-by-4	600 sec. (10 min.)	1.72 sec.

Because the port setup in HFSS uses wave-port model, the reference admittance Y_{0i} at each port is calculated using infinite transmission line model with the cross section geometry as defined by the antipad and pad. Since $LC = \mu\epsilon$ for the fundamental TEM wave in the general transmission line, we can calculate L , the inductance per unit length, from C . Then Y_{0i} is obtained by using $Y_{0i} = \sqrt{C/L}$.

IV. NUMERICAL RESULTS AND DISCUSSION

All the numerical examples here are using the following specifications: $\epsilon_r = 4$, $R_{\text{via}} = 5$ mil, $R_{\text{pad}} = 10$ mil, $R_{\text{antipad}} = 15$ mil, pitch = 42 mil, $h = 30$ mil. Fig. 4 shows the insertion loss and the return loss for both a via at a corner and a via near the center of the 4-by-4 via array with center drilling as well as with 4 mil off-center drilling (see Figs. 1(a) and 3).

The center via has more neighboring vias than the corner via, which means a smaller change of impedance along the via. On the other hand, a via at the corner has more power being radiated away whereas a via at the center is shielded by vias all around. Thus the center via has better signal propagation. Comparing the results between center drilling and off-center drilling, we notice that off-center drilling has about 0.2 dB less insertion loss and about 1 dB more return loss at 20 GHz due to the larger parasitic capacitance in narrowed space. Our results compare well with the results of HFSS for all the cases. The required CPU is reported using Matlab on Intel Qual-core 3.0 GHz processor 13 GB RAM and compared with HFSS in Table I. The non-concentric cylinder case can be calculated by an analytic two-wire approach [8]. However, the FDM has the advantage that it can handle general arbitrary shape of antipad and pad. The CPU using numerical FDM is slightly more than the run time of analytic approach [8].

Fig. 5 shows results on top ports of the 8-by-8 center drilling via array in circular antipads on top plane and squared antipads on bottom plane [see Fig. 1(b)]. The side of square L_{side} is 30 mil. Since the top ports are different from bottom ports, hence using notations in [3], [4], $\mathbf{Y}^{uu} \neq \mathbf{Y}^{bb}$, $\mathbf{Y}^{bu} \neq \mathbf{Y}^{ub}$, and $\mathbf{S}^{uu} \neq \mathbf{S}^{bb}$. Yet \mathbf{S} is a unitary matrix in the reciprocal and lossless networks

$$\begin{bmatrix} I^u \\ -I^b \end{bmatrix} = - \begin{bmatrix} Y^{uu} & Y^{ub} \\ Y^{bu} & Y^{uu} \end{bmatrix} \begin{bmatrix} -V^u \\ V^b \end{bmatrix} \quad (6)$$

$$\mathbf{S} = (\mathbf{Y}_0 + \mathbf{Y})^{-1}(\mathbf{Y}_0 - \mathbf{Y}) \quad (7)$$

where \mathbf{Y}_0 is a diagonal matrix with each element of port i using the port admittance Y_{0i} individually. Comparing with the results of all circular antipads in Fig. 4, we notice that the bigger the aperture, the better the signal propagates due to the less parasitic capacitance between via to ground/power plates.

Fig. 6 shows results of the 8-by-8 center drilling via array with circular pads and circular antipads on both planes [see Fig. 1(c)].

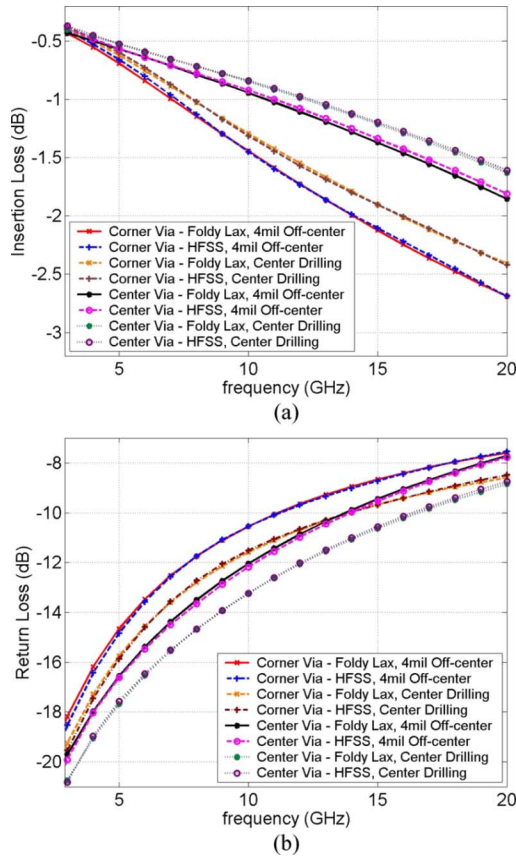


Fig. 4. (a) Insertion loss, and (b) return loss of 4-by-4 via array for both center drilling and 4 mil off-center drilling without via-pad.

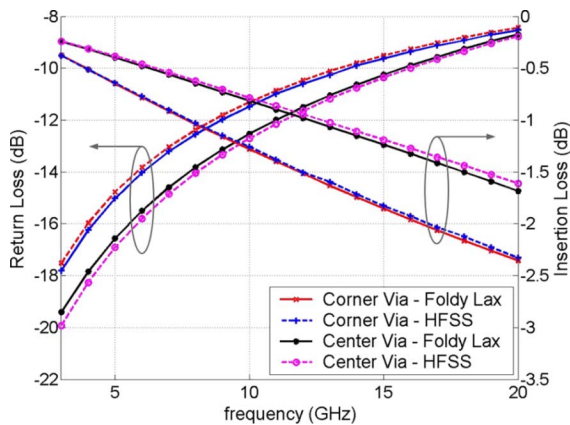


Fig. 5. Insertion loss and return loss on top ports of 8-by-8 via array with circular antipads on top and squared antipads at bottom, but without via-pad.

The signal performance of via-pad structure in Fig. 6 is significantly poorer than those without via-pad in Fig. 4, mainly because of the additional parasitic capacitances at the pads. The results of Foldy-Lax approach are within 5% difference of the results from HFSS. Note that the CPU of Foldy-Lax approach for the case of 16-by-16 via array is about five thousand times faster than HFSS as shown in Table I.

In order to show the significant differences of signal performance when changing the configurations of the pads and antipads, we present cases of relative thin substrate that emphasize

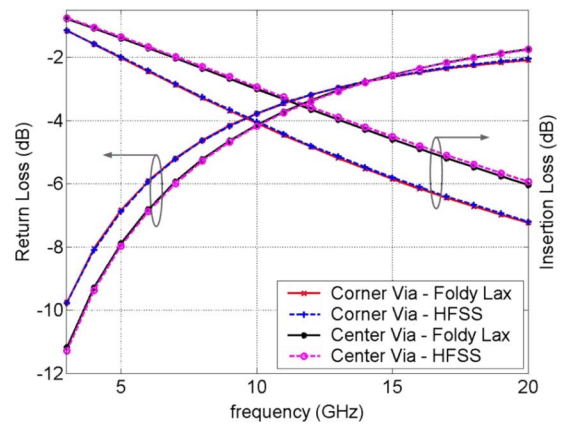


Fig. 6. Insertion loss and return loss of 8-by-8 via array with circular pads and circular antipads on both planes.

higher capacitance and lower radiation. We analyzed the conductor loss and dielectric loss in our past work [9]. In this letter, we do not include any loss and all the metals are assumed PEC. For the special port structure when fundamental TEM wave does not greatly dominate, we can include the higher order modes in future studies.

ACKNOWLEDGMENT

The authors wish to thank D. Miller and T.G. Ruttan, Intel Corporation, and X. Gu, IBM Corporation, for useful discussions and support.

REFERENCES

- [1] E. Laermans, J. De Geest, D. De Zutter, F. Olyslager, S. Sercu, and D. Morlion, "Modeling complex via hole structures," *IEEE Trans. Adv. Packag.*, vol. 25, no. 2, pp. 206–214, May 2002.
- [2] Q. Gu, M. A. Tassoudji, S. Y. Poh, R. T. Shin, and J. A. Kong, "Coupled noise analysis for adjacent vias in multilayered digital circuits," *IEEE Trans. Circuits Syst.*, vol. 41, no. 12, pp. 796–804, Dec. 1994.
- [3] L. Tsang, H. Chen, C.-C. Huang, and V. Jandhyala, "Modeling of multiple scattering among vias in planar waveguides using Foldy-Lax equations," *Microw. Opt. Technol. Lett.*, vol. 31, no. 3, pp. 201–208, Nov. 2001.
- [4] L. Tsang, H. Chen, C.-C. Huang, and V. Jandhyala, "Methods for Modeling Interactions Between Massively Coupled Multiple Vias in Multilayered Electronic Packaging Structures," U.S. Patent 7 149 666, Dec. 12, 2006.
- [5] C.-J. Ong, D. Miller, L. Tsang, B. Wu, and C.-C. Huang, "Application of the Foldy-Lax multiple scattering method to the analysis of vias in ball grid arrays and interior layers of printed circuit boards," *Microw. Opt. Technol. Lett.*, vol. 49, no. 1, pp. 225–231, Jan. 2007.
- [6] X. Gu and M. B. Ritter, "Application of Foldy-Lax multiple scattering method to via analysis in multi-layered printed circuit board," in *Proc. DesignCon'08*, Santa Clara, CA, Feb. 4–Feb. 7 2008, [CD ROM].
- [7] Z. Z. Oo, E.-X. Liu, E.-P. Li, X. Wei, Y. Zhang, M. Tan, L.-W. Li, and R. Vahldieck, "A semi-analytical approach for system-level electrical modeling of electronic packages with large number of vias," *IEEE Trans. Adv. Packag.*, vol. 31, no. 2, pp. 267–274, May 2008.
- [8] R. Rimolo-Donadio, H.-D. Brüns, and C. Schuster, "Analytical Solution for Offset via Capacitance and Fields," Institut für Theoretische Elektrotechnik, Technische Universität Hamburg-Harburg, Hamburg, Germany, Feb. 2008.
- [9] C. C. Huang, L. Tsang, and C. H. Chan, "Multiple scattering among vias in lossy planar waveguides using SMCG method," *IEEE Trans. Adv. Packag.*, vol. 25, no. 2, pp. 181–188, May 2002.